

Batch statistical process control of a fluid bed granulation process using in-line spatial filter velocimetry and product temperature measurements

A. Burggraeve<sup>a\*</sup>, T. Van Den Kerkhof<sup>b</sup>, M. Hellings<sup>b</sup>, J.P. Remon<sup>c</sup>, C. Vervaet<sup>c</sup>, T. De Beer<sup>a</sup>

<sup>a</sup>Laboratory of Pharmaceutical Process Analytical Technology, Department of Pharmaceutical Analysis, Ghent University, Harelbekestraat 72, B-9000 Ghent, Belgium

<sup>b</sup>Johnson & Johnson Pharmaceutical Research and Development, Analytical Development, Turnhoutseweg 30, B-2340 Beerse, Belgium

<sup>c</sup>Laboratory of Pharmaceutical Technology, Department of Pharmaceutics, Ghent University, Harelbekestraat 72, B-9000 Ghent, Belgium

\*Corresponding author:

Anneleen Burggraeve  
Harelbekestraat 72  
B-9000 Ghent  
Belgium  
Tel: +32 9 264 83 55  
Fax: +32 9 222 82 36  
Email: [anneleen.burggraeve@ugent.be](mailto:anneleen.burggraeve@ugent.be)

## Abstract

Fluid bed granulation is a batch process, which is characterized by the processing of raw materials for a predefined period of time, consisting of a fixed spraying phase and a subsequent drying period. The present study shows the multivariate statistical modeling and control of a fluid bed granulation process based on in-line particle size distribution (PSD) measurements (using spatial filter velocimetry) combined with continuous product temperature registration using a partial least squares (PLS) approach. Via the continuous in-line monitoring of the PSD and product temperature during granulation of various reference batches, a statistical batch model was developed allowing the real-time evaluation and acceptance or rejection of future batches.

Continuously monitored PSD and product temperature process data of 10 reference batches (X-data) were used to develop a reference batch PLS model, regressing the X-data versus the batch process time (Y-data). Two PLS components captured 98.8% of the variation in the X-data block. Score control charts in which the average batch trajectory and upper and lower control limits are displayed were developed. Next, these control charts were used to monitor 4 new test batches in real-time and to immediately detect any deviations from the expected batch trajectory. By real-time evaluation of new batches using the developed control charts and by computation of contribution plots of deviating process behavior at a certain time point, batch losses or reprocessing can be prevented.

Immediately after batch completion, all PSD and product temperature information (i.e., a batch progress fingerprint) was used to estimate some granule properties (density and flowability) at an early stage, which can improve batch release time. Individual PLS models relating the computed scores (X) of the reference PLS model (based on the 10 reference batches) and the density, respectively flowability as Y-matrix, were developed. The scores of the 4 test batches were used to examine the predictive ability of the model.

## Keywords

fluid bed granulation, spatial filter velocimetry, particle size distribution, batch process modeling, process analytical technology, multi-way analysis

## 1. Introduction

A fluid bed granulation batch process consists of successive spraying and drying phases to create larger permanent aggregates or granules in which the original particles are still identifiable (Iveson et al., 2001). A batch process is generally characterized by a predefined processing of raw materials for a *finite* period of time. The granulation process itself is also complex due to many interrelated variables (such as inlet air relative humidity and temperature, fluidizing air flow rate, atomization pressure, spray rate, etc) and it is susceptible to natural, random variations in process and formulation variables which can cause significant batch-to-batch variations. However, a high degree of reproducibility is necessary to obtain successful batches that meet the quality requirements. Traditionally, final product quality is assessed off-line by a number of quality evaluations on end product samples. If these end product quality properties do not meet the predefined criteria, the entire batch is rejected or reprocessed. Moreover, identification of failure cause and prevention of batch failure by real-time adjustments to the process is most difficult or even impossible when using this traditional off-line evaluation. This can be prevented through in-line measurements of critical quality parameters and statistical control of the batch process. Using this approach, processing of material via fluid bed granulation is not marked by a predefined duration of time, but the endpoint of the granulation process is defined by the in-line measured end product quality.

Particle size distribution (PSD) is considered as one of the main quality attributes of a granulated product as it influences other granule properties such as density, powder flow and compression. Hence, the change in PSD during granulation gives a direct indication of the batch progress and batch quality. Several techniques have been evaluated to monitor PSD during granulation in real-time: near infrared spectroscopy (Alcala et al., 2010; Findlay et al., 2005; Frake et al., 1997; Goebel and Steffens, 1998; Kaddour and Cuq, 2009; Luukkonen et al., 2008; Tok et al., 2008), focused beam reflectance method (Hu et al., 2008; Huang et al., 2010; Tok et al., 2008), spatial filter velocimetry (SFV) (Burggraeve et al., 2010; Lipsanen et al., 2008; Narvanen et al., 2008, 2009), image analysis (Laitinen et al., 2004; Naervanen et al., 2008; Watano and Miyanami, 1995; Watano et al. 1996, 1997, 2000, 2001; Watano, 2001) and acoustic emission monitoring (AE) (Gamble et al., 2009; Halstensen et al., 2006; Matero et al., 2009; Tok et al., 2008; Whitaker et al., 2000). Each technique has its own advantages and shortcomings. Usually, the main challenge is to find the appropriate position of probes and lenses in the process stream to perform representative measurements and to prevent fouling. Fouling is not a problem when using non-intrusive AE measurements. However, as the AE signals are usually weak, external uncontrollable factors and the fluidizing airflow rate may influence the technique's sensitivity.

In this study, SFV was used in-line during top-spray fluid bed granulation to continuously obtain PSD information. The SFV technique measures simultaneously the velocity and the chord length distribution of particles as they pass through the laser light and cast a shadow onto the detector (Petрак, 2002; Petрак and Rauh, 2006). The measurement cell of the SFV probe is equipped with sapphire windows that are kept clean via an internal compressed air supply system, preventing window fouling. A previous study has shown that the technique is sensitive to any particle size changes during fluid bed granulation (Burggraeve et al., 2010). Hence, the sensitivity of the technique combined with the short measuring time make SFV an appropriate tool to continuously gather PSD information throughout a granulation process. SFV data were combined with a continuous registration of the product temperature to model and statistically control the fluid bed

granulation process using a partial least squares (PLS) approach. The 3-way data matrix [*batch x variable (in this study: PSD and product temperature) x batch process time*] comprising process and product information of 10 reference batches (i.e., good batches) was unfolded to new matrices, suitable for PLS analysis (figure 1). The resulting reference model was used to indicate possible deviations from process normality and to detect the process endpoint for new in-line monitored batches (4 test batches). Hence, the reference batch model allows direct process and product quality evaluation and permits early fault diagnosis. Full PSD and product temperature information of completed granulation batches was used to estimate density and flowability at an early stage, immediately after batch production. Individual PLS models relating the computed scores (X) of the reference PLS model and these granule properties (Y-matrix) were built.

## 2. Materials and Methods

### 2.1. Materials

The powder mixture used during all granulations consisted of 700 g dextrose monohydrate (Roquette Frères, Lestrem, France) and 272.5 g unmodified maize starch (Cargill Benelux, Sas van Gent, The Netherlands). The powder mass was granulated with an aqueous binder solution of 25 g HPMC (type 2910 15 mPa s, Dow Chemical Company, Plaquemine, LA, USA) and 2.5 g Tween 20 (Croda Chemicals Europe, Wilton, UK) resulting into a total amount of solids of 1000 g for each batch. HPMC was always sprayed as a 4% solution.

### 2.2. Fluid bed granulation set-up

Granulations were performed in a laboratory scale fluid bed granulator (GPCG 1, Glatt, Binzen, Germany). A nozzle with a diameter of 1.2 mm was installed top-spray at a height of 26 cm from the distributor plate, and an atomization pressure of 1 bar was used during all experiments. For the 10 reference batches, granulation liquid was sprayed at a rate of 16 g/min, inlet air velocity was set to 8 m/s and shaking of the filter bags was performed every 45 s for a period of 7 s. The inlet air temperature during spraying and drying was 45°C and 60°C, respectively. Granules were dried until an outlet air temperature of 37°C and a product temperature of 45°C was obtained.

A spatial filter velocimetry probe (Parsum IPP 70; Gesellschaft für Partikel-, Strömungs- und Umweltmesstechnik, Chemnitz, Germany) was installed in the fluid bed granulator at a height of 20 cm from the distributor plate and at approximately 5 cm from the sidewall of the granulator. Particles passed through an aperture with 4 mm diameter and a pressurized air connection was used to disperse the particles and prevent fouling of the measurement zone. Measured raw data were collected via an A/D converter. The software (In-line Particle Probe V7.12a) operated in the Windows XP environment. The experimental set-up and software settings were based on the knowledge of a previous study (Burggraeve et al., 2010).

During the entire top-spray granulation processes, an average PSD was saved every 10 s and product temperature values were registered every minute. The batch model was developed using the PSD and product temperature values continuously obtained during processing of the reference batches (i.e. 10 batches with identical process and formulation settings; see 2.4.). Four test batches (TB A-D) were performed to evaluate the batch process model (table 1). The process settings of TB B-D deviated from the reference batches and represented typical errors occurring during fluid bed granulation processes. For example, the blockage of tubing was simulated by interruption of liquid spraying and overwetting of granules was simulated by the use of a higher feed rate.

### 2.3. Characterization of granules

After manufacturing, bulk density, tapped density and Hausner ratio of the end product of each batch were determined. Approximately 30 g samples were gently poured into a 100 mL graduated cylinder. The granule weight and volume were used to calculate bulk density. Next, each sample was tapped 1250 times using an automatic tapper (J. Engelsmann AG, Ludwigshafen am Rhein, Germany) and the new volume was used to determine the tapped density. All density measurements were performed in triplicate and the average density was calculated. Bulk and tapped densities were used to determine powder flow characteristics via calculation of Hausner ratio values.

### 2.4. Development of batch model

The batch process model was developed and evaluated using the SIMCA-P+ software (Version 12.0.1, Umetrics, Umeå, Sweden).

During each granulation process,  $J$  variables (product temperature and particle sizes  $D_{01}$ ,  $D_{10}$ ,  $D_{25}$ ,  $D_{50}$ ,  $D_{63}$ ,  $D_{75}$ ,  $D_{90}$ ,  $D_{99}$ , expressing which percentile of the PSD has a PS smaller than this value) were measured at  $K$  time points. Consequently, a set of  $N$  batches resulted into a 3-way granulation data matrix  $X$  with dimensions  $N \times J \times K$  (figure 1, left). Initially, the 3-way batch data matrix was unfolded in such a way that the direction of the  $J$  variables was preserved. In the resulting 2-way matrix  $X_A$  (figure 1, middle), the batch and time dimensions are combined, creating a matrix with  $N \times K$  observations (rows) and  $J$  variables (columns). Hence, each row in  $X_A$  represents the data of batch  $N$  at time point  $K$  for variable  $J$ . A dummy  $Y_A$  vector having a length of  $N \times K$  and expressing the local batch time was autogenerated by the software. Partial least squares regression was performed relating  $X_A$  and  $Y_A$ . The correct number of PLS components (PLSC) was based on cross validation, using the approach of Krzanowski (Eastment and Krzanowski, 1982). The value of local time predicted by the reference PLS model indicates the maturity of a batch (i.e., how far the batch has evolved over time).

In a next step, score control charts were established to identify the characteristic trajectory of a reference batch. These charts were then used to monitor the evolution of the test batches in real-time. The score control charts were developed by rearranging the scores of each PLSC, resulting in a new matrix per PLS component in which each row corresponds to the scores of one batch (figure 2, left:  $X_{A1}$ ,  $X_{A2}$ , ...). Consequently, these matrices have  $N$  rows and  $K$  columns. From these matrices the averages and standard deviations (SD) of each series of scores (each column) were calculated (figure 2, right). Hence, score control charts were obtained for each PLS component with control intervals set to average  $\pm 3$  SD (Shewhart, 1931). The use of 3 SD ensures that 99.7% of the variation in the accepted reference batches lies within the control limits. The data of the 4 test batches (table 1) were then projected onto the reference PLS model, allowing the computation of their respective score values. These score values were plotted in the control charts and the quality of the test batch trajectory was compared to the trajectories of the reference batches (i.e., score trajectory is within or outside the control interval).

After granulation completion, all PSD and product temperature data collected during the production of the 10 reference batches were used to make a principal component analysis (PCA) model. However, instead of the original measured PSD and product temperature values, the scores of the reference batch PLS model ( $X_B$  matrix) were used (figure 3). PSD and product temperature

information gathered during processing of the 4 test batches were used as a prediction set. In that way, the quality of the test batches could be determined (i.e. batch acceptance or rejection). Finally, PLS regression was performed to relate the measured process information ( $X_B$ ) to 3 end product characteristics (i.e., bulk density, tapped density and Hausner ratio;  $Y_B$ ), hence allowing to predict the final product quality of new batches from the PSD and product temperature evolution during granulation. In that way, time consuming off-line analysis might become unnecessary.

### 3. Results and Discussion

#### 3.1. Real-time batch progress evaluation

The training set consisting of the in-line collected PSD and product temperature data for 10 reference batches was unfolded and the resulting 2-way  $X_A$  matrix was regressed versus the batch process time ( $Y_A$  matrix) using PLS (figure 1). A reference model with 2 significant PLS components was developed corresponding to  $R^2X$  (cum) = 0.988,  $Q^2$  (cum) = 0.967 and RMSEE = 2.5 min. The  $R^2X$  value expresses that 98.8% of the variation in  $X_A$  was captured by the model. The significance of  $Q^2$  (goodness of prediction) should not be overestimated as the  $Y_A$  matrix was artificially generated. The PLS score scatter plot of the 2-component reference PLS model (figure 4) demonstrates that all reference batches had a similar score trajectory. Hence, no deviating reference batches were detected. The scores of all batches initialized in the upper left quadrant (negative  $t_1$ , positive  $t_2$ ) and finished in the upper right quadrant (positive  $t_1$ , positive  $t_2$ ). In addition, the plot shows that the first PLSC reflected the evolution of PSD of a normal batch in function of time: growth (increase in  $t_1$  value) and attrition (decrease in  $t_1$  value) of granules. The second component described the difference between the spraying and the drying phase. During spraying, the product temperature decreased until it reached a minimum value (22°C - 23°C). Subsequently, during drying the product temperature increased. This interpretation of the 2 PLS components was confirmed by the corresponding loading plots (figures 5a and 5b show the loading column plots for the 1<sup>st</sup> and 2<sup>nd</sup> PLSC, respectively). All particle size fractions contributed strongly to the 1<sup>st</sup> component, while the product temperature only contributed to the 2<sup>nd</sup> component.

In a next step, the scores of the reference model were rearranged to develop score control charts for each PLS component in which the average batch trajectory with an upper and lower control limit in function of process time is displayed (section 2.4 and figure 2). The scores of all training set batches lay between the calculated control limits in the resulting control charts (figures 6a and 6b), confirming previous results that there were no outliers in the set of reference batches. A clear distinction between the spraying and drying period is visible in both charts.

The established reference model was then used to monitor the evolution of 4 test batches (table 1), and the resulting score control charts are displayed in figures 7a-d. In these charts, score values of completed test batches are shown. In practice however, the calculated scores of ongoing batches can be projected in real-time into these plots even though all data has not yet been determined.

**Test batch A** was performed under identical conditions as the reference batches. The scores of this batch behaved similar as the average score values of the reference batches and were hence within the set control limits in each score control chart throughout the whole process (figures 7a and 7c).

The pump used to spray the granulation liquid during the spraying phase was stopped for one and nine minutes in **test batch B and C**, respectively, hence simulating a blockage of the tubing. For **test**

**batch B**, this resulted into an immediate fluctuation of the PLSC1 scores (figure 7a) and an increase in PLSC2 scores (figure 7c). When interrupting the spraying of the granulation liquid, the already shaped agglomerates dried and created fines due to attrition of the granules. As these fines were trapped in the filter bags, these small particles were released when the bags were shaken every 45 s, which caused a drop in PS value and hence more fluctuations on PLSC1 scores. Furthermore, due to drying of the granules during the interruption of spraying, the product temperature increased resulting in higher PLSC2 scores. When liquid spraying was restarted after one minute, the fines adhered to larger granules resulting in less fluctuations in particle size (i.e., PLSC1 scores, figure 7a) and a lower product temperature (PLSC2 scores, figure 7c). During the next stage of the spraying phase and the subsequent drying phase, the scores for both components were similar to the average trajectory and the influence of a 1 minute liquid feeding interruption was negligible at the end of the granulation process. The scores of **test batch C** (interruption of liquid spraying for 9 minutes) showed a similar pattern: fluctuation on PLSC1 scores (figure 7b) and an increase in PLSC2 scores (figure 7d). However, the scores for both components progressed outside the control limits. When spraying was restarted after nine minutes, the agglomeration process continued and the PLSC1 and PLSC2 scores evolved towards the average trajectory. At the end of the granulation process, PLSC1 scores were close to the lower control limit, indicating a batch of low quality. During the 9 minutes pause of liquid feeding, the PSD of the granules decreased extensively. Although a total identical amount of liquid was sprayed compared to the reference batches, this was not sufficient to ensure a similar particle size at the end of the granulation process. If this phenomenon would occur during routine production, it could possibly be prevented by increasing the amount of binder liquid sprayed onto the powder bed or increasing the granulation feed rate until PLSC1 scores similar to the average values of the reference batches are obtained (Narvanen et al., 2008). Based on the PLSC2 scores, this batch showed a normal drying period.

The liquid feed rate of **test batch D** was increased to 21 g/min. Already during the early stages of the process the PLSC1 and PLSC2 scores were outside the control interval and throughout the entire granulation process the scores of PLSC1 were above the upper control limit (figures 7b and 7d). At a higher liquid addition rate, liquid saturation of the powder bed increased (consequently the growth rate of the granules was faster, as reflected in the PLSC1 scores) and the granule temperature was lower (as reflected in the PLSC2 scores) compared to the average batch trajectory. The higher feed rate created granules with more liquid bridges and with stronger cohesive forces which prevented breakage of the granules during drying (constant PLSC1 scores during drying phase, figure 7b). As binder liquid was sprayed at a faster rate, drying of granules initiated earlier and due to the higher moisture content, drying extended over a longer period.

Evaluation of test batches data using the score control charts showed that the developed PLS model allowed the real-time detection of deviations from the normal batch trace. Even when the granulation feeding was interrupted during a single minute, this problem was instantly detected in both control charts, hence permitting early fault diagnosis.

In this study, particle size and product temperature information were gathered during processing. This resulted in a 2 PLS component model describing 98.8% of the variation in the process data. However, when monitoring more variables in complex systems (e.g., during fluid bed granulation: pressure difference over the filter; temperature, relative humidity and flow rate of inlet/outlet air; etc.), the use of a larger number of PLS components might be needed to model the evolution of the batches. As the use of many individual score control charts might then become cumbersome, a

statistic called Hotelling's  $T^2$  can be calculated enabling to monitor and evaluate the overall performance of a new batch with a single chart. In the Hotelling's  $T^2$  plot the distance from the origin in the score space of the reference PLS model for each selected observation of a test batch is displayed and the  $T^2$  values are calculated for the 2 PLSC selected. Figures 8a and 8b display the corresponding Hotelling's  $T^2$  plots for test batches A-B and C-D respectively. The average reference batch trajectory is displayed in green and deviations can be immediately detected. The 95% confidence limit was not exceeded for test batch A, and only for a limit period for test batch B, indicating that no deviations for PSD and product temperature (compared to the reference batches) were measured during processing of these test batches. In contrast, in the Hotelling's  $T^2$  plot of test batch C and D,  $T^2$  values differed significantly from the  $T^2$  values of the reference model (similar observations based on the score control charts, figures 7b and 7d). Hence, PLS score control charts and Hotelling's  $T^2$  plots can both be used to monitor new batches. Based on these different types of charts, same observations can be made. The choice of chart type depends on the examiner's preference.

When detecting deviations from the normal batch trajectory in the Hotelling's  $T^2$  plot, it is possible to identify the monitored variable(s) responsible for this difference through the computation of contribution plots (Wold et al., 1998). A contribution plot displays the differences between the outlying observation and average observation for each **monitored** variable **in the model**. Information from a previously performed design of experiments (DoE) can sometimes be used to correctly adjust process variables and lead the scores towards the average direction. The use of contribution plots is exemplified in figures 9a-c for test batch C. At time point 125 (figure 9a) both PSD and product temperature showed a similar deviation from the average observation due to the interruption of spraying prior to this time point. One minute and 40 seconds later (time point 135, figure 9b), the deviation was mainly determined by the high product temperature. After restarting of liquid spraying (time point 165, figure 9c), the product temperature recovered rapidly to the average observation while not all fines could adhere to the larger granules. In a previous study, the influence of process and formulation variables upon the PSD of this formulation was studied in a DoE, which showed that the amount of HPMC had a positive effect upon granule size (Burggraeve et al., 2010). A possible action to prevent batch failure due to the large amount of fines, might for example be to spray more HPMC until the scores correspond to the average value. In practice, the granulation kinetics should also be taken into consideration as they might be influenced by the addition of larger HPMC amounts.

### 3.2. Evaluation of completed batches

The scores of the reference PLS model (modelling the 10 reference batches, section 3.1) were rearranged to form a new X-data matrix consisting of 10 rows and 2 PC\*time columns ( $X_B$  matrix, figure 3). Hence, each row corresponded to one batch. Without the use of an external y-variable, principal component analysis was performed on the  $X_B$ -data block. The resulting PCA model consisted of 3 principal components, capturing 77% of the total batch process variation. The PCA score plot shows a homogeneous distribution among the 10 reference batches (figure 10, B1 – B10) indicating the absence of any deviating batches among the reference set. The developed PCA batch model was then used to classify the 4 test batches. Figure 10 indicates that 2 test batches (TB A and B) were within the confidence ellipse at a significance level of 0.05 and thus of a quality similar to the reference batches. Test batches C and D were outside the confidence ellipse, having a minor product quality. Based on the score control charts in figures 7a-d, similar conclusions were made for test

batches A, B and D. In both score control charts the scores of test batch C were at the end of the process within the control interval. However, based on the whole batch performance, the final batch quality is unacceptable.

The granule quality attributes bulk density, tapped density and Hausner ratio were determined after completion of each reference and test batch. A PLS model was developed to relate the reference  $X_B$  data matrix to these final product characteristics as response variables (figure 3). This model was then used to predict the final product characteristics of the test batches (table 2) based on their in-line collected PSD and product temperature information. Models with RMSEP values of 0.034 g/ml, 0.036 g/ml and 0.022 for bulk density, tapped density and Hausner ratio were established. The final product bulk density, tapped density and Hausner ratio of test batches A and B were similar to the quality of the reference batches and showed a good predictability by the PLS model. Density and Hausner ratio of test batches C and especially D deviated from the reference batches. Hence, the difference between the measured and predicted granule properties was larger for these batches. This use of PLS to relate monitored process and product values of good batches (good/bad classification based on previous score trajectories (figures 7 and 8) and PCA analysis (figure 10)) to end product characteristics allows the early estimation of these properties immediately after production. Hence, traditional time-consuming off-line analysis becomes superfluous.

#### 4. Conclusions

The objective of this study was to model and control a fluid bed granulation process based on in-line particle size distribution measurements combined with continuous product temperature registration. A PLS model of 10 reference batches allowed to evaluate the process and product quality of 4 new test batches. In the developed control charts, the scores of complete batches were shown. However, in practice these control charts can be used for ongoing batches, even though all data have not yet been determined. As the reference model was sensitive to small process deviations, the presented approach of real-time monitoring of a fluid bed granulation process allowed early fault detection. This tool can be used to improve process efficiency and to reduce batch reprocessing and/or batch loss.

The use of full batch information after batch completion allowed to estimate important product characteristics (i.e., density and flowability) at an early stage. This may reduce the lag period between the end of the granulation process and downstream processing, when granules are held for laboratory testing.

#### Acknowledgement

This work was financially supported by the Institute for the Promotion of Innovation through Science and Technology in Flanders (IWT-Vlaanderen).

#### References

- Alcala, M., Blanco, M., Bautista, M., Gonzalez, J.M., 2010. On-Line monitoring of a granulation process by NIR spectroscopy. *J. Pharm. Sci.* 99, 336-345.
- Burggraeve, A., Van Den Kerkhof, T., Hellings, M., Remon, J.P., Vervaet, C., De Beer, T., 2010. Evaluation of in-line spatial filter velocimetry as PAT monitoring tool for particle growth during fluid bed granulation. *Eur. J. Pharm. Biopharm.* 76, 138-146.
- Eastment, H., Krzanowski, W., 1982. Crossvalidatory choice of the number of components from a principal component analysis. *Technometrics* 24, 73-77.
- Findlay, W.P., Peck, G.R., Morris, K.R., 2005. Determination of fluidized bed granulation end point using near-infrared spectroscopy and phenomenological analysis. *J. Pharm. Sci.* 94, 604-612.
- Frake, P., Greenhalgh, D., Grierson, S.M., Hempenstall, J.M., Rudd, D.R., 1997. Process control and end-point determination of a fluid bed granulation by application of near infra-red spectroscopy. *Int. J. Pharm.* 151, 75-80.
- Gamble, J.F., Dennis, A.B., Tobyn, M., 2009. Monitoring and end-point prediction of a small scale wet granulation process using acoustic emission. *Pharm. Dev. Technol.* 14, 299-304.
- Goebel, S.G., Steffens, K.J., 1998. On-line measurement of moisture and particle size in the fluidized-bed processing with the near-infrared spectroscopy. *Pharm. Ind.* 60, 889-895.
- Halstensen, M., de Bakker, P., Esbensen, K.H., 2006. Acoustic chemometric monitoring of an industrial granulation production process - a PAT feasibility study. *Chemometr. Intell. Lab. Syst.* 84, 88-97.
- Hu, X.H., Cunningham, J.C., Winstead, D., 2008. Study growth kinetics in fluidized bed granulation with at-line FBRM. *Int. J. Pharm.* 347, 54-61.
- Huang, J., Kaul, G., Utz, J., Hernandez, P., Wong, V., Bradley, D., Nagi, A., O'Grady, D., 2010. A PAT approach to improve process understanding of high shear wet granulation through in-line particle measurement using FBRM C35. *J. Pharm. Sci.* 99, 3205-3212.
- Iveson, S.M., Litster, J.D., Hapgood, K., Ennis, B.J., 2001. Nucleation, growth and breakage phenomena in agitated wet granulation processes: a review. *Powder Technol.* 117, 3-39.
- Kaddour, A.A., Cuq, B., 2009. In line monitoring of wet agglomeration of wheat flour using near infrared spectroscopy. *Powder Technol.* 190, 10-18.
- Laitinen, N., Antikainen, O., Rantanen, J., Yliruusi, J., 2004. New perspectives for visual characterization of pharmaceutical solids. *J. Pharm. Sci.* 93, 165-176.
- Lipsanen, T., Narvanen, T., Raikkonen, H., Antikainen, O., Yliruusi, J., 2008. Particle Size, moisture, and fluidization variations described by indirect in-line physical measurements of fluid bed granulation. *AAPS Pharm. Sci. Technol.* 9, 1070-1077.
- Luukkonen, P., Fransson, M., Bjorn, I.N., Hautala, J., Lagerholm, B., Folestad, S., 2008. Real-time assessment of granule and tablet properties using in-line data from a high-shear granulation process. *J. Pharm. Sci.* 97, 950-959.

- Matero, S., Poutiainen, S., Leskinen, J., Jarvinen, K., Ketolainen, J., Reinikainen, S.P., Hakulinen, M., Lappalainen, R., Poso, A., 2009. The feasibility of using acoustic emissions for monitoring of fluidized bed granulation. *Chemometr. Intell. Lab. Syst.* 97, 75-81.
- Naervanen, T., Seppaelae, K., Antikainen, O., Yliruusi, J., 2008. A new rapid on-line imaging method to determine particle size distribution of granules. *AAPS Pharm. Sci. Technol.* 9, 282-287.
- Narvanen, T., Lipsanen, T., Antikainen, O., Raikkonen, H., Yliruusi, J., 2008. Controlling granule size by granulation liquid feed pulsing. *Int. J. Pharm.* 357, 132-138.
- Narvanen, T., Lipsanen, T., Antikainen, O., Raikkonen, H., Heinamaki, J., Yliruusi, J., 2009. Gaining Fluid Bed Process Understanding by In-Line Particle Size Analysis. *J. Pharm. Sci.* 98, 1110-1117.
- Petrak, D., 2002. Simultaneous measurement of particle size and particle velocity by the spatial filtering technique. *Part. Part. Syst. Charact.* 19, 391-400.
- Petrak, D., Rauh, H., 2006. Optical probe for the in-line determination of particle shape, size, and velocity. *Part. Sci. Technol.* 24, 381-394.
- Shewhart, W., 1931. *Economic control of quality of manufactured product.* Van Nostrand, Princeton, N.J.
- Tok, A., Goh, X.P., Ng, W., Tan, R., 2008. Monitoring granulation rate processes using three PAT tools in a pilot-scale fluidized bed. *AAPS Pharm. Sci. Technol.* 9, 1083-1091.
- Watano, S., Miyanami, K., 1995. Image-processing for online monitoring of granule size distribution and shape in fluidized-bed granulation. *Powder Technol.* 83, 55-60.
- Watano, S., Sato, Y., Miyanami, K., 1996. Control of granule growth in fluidized bed granulation by an image processing system. *Chem. Pharm. Bull.* 44, 1556-1560.
- Watano, S., Sato, Y., Miyanami, K., 1997. Optimization and validation of an image processing system in fluidized bed granulation. *Adv. Powder Technol.* 8, 269-277.
- Watano, S., Numa, T., Miyanami, K., Osako, Y., 2000. On-line monitoring of granule growth in high shear granulation by an image processing system. *Chem. Pharm. Bull.* 48, 1154-1159.
- Watano, S., 2001. Direct control of wet granulation processes by image processing system. *Powder Technol.* 117, 163-172.
- Watano, S., Numa, T., Miyanami, K., Osako, Y., 2001. A fuzzy control system of high shear granulation using image processing. *Powder Technol.* 115, 124-130.
- Whitaker, M., Baker, G.R., Westrup, J., Goulding, P.A., Rudd, D.R., Belchamber, R.M., Collins, M.P., 2000. Application of acoustic emission to the monitoring and end point determination of a high shear granulation process. *Int. J. Pharm.* 205, 79-91.
- Wold, S., Kettaneh, N., Friden, H., Holmberg, A., 1998. Modelling and diagnostics of batch processes and analogous kinetic experiments. *Chemometr. Intell. Lab. Syst.* 44, 331-340.

Figure 1. Schematic overview of the unfolding of the 3-way batch data matrix preserving variable direction.

Figure 2. Schematic overview of the PLS scores rearrangement (shown for the first 2 PLS components) and calculation of averages and standard deviations (SD) to develop score control charts.

Figure 3. Schematic overview of the scores rearrangement to model whole batches. Initially, PCA was performed on  $X_B$  and in a next step PLS analysis was used to regress the  $X_B$ -matrix to end product properties contained in the  $Y_B$ -matrix.

Figure 4. PLS  $t_1/t_2$  score scatter plot of the initial PLS model for all 10 reference batches .

Figure 5. Loading column plot of the 1<sup>st</sup> PLS component (a) and 2<sup>nd</sup> PLS component (b).

Figure 6. Batch control charts for PLSC 1 (a) and PLSC 2 (b). Average batch trajectory, upper and lower control limits (CL) and the observed trajectories of the ten reference batches (B1 – B10) are shown.

Figure 7. Batch prediction control charts for PLSC 1 (a-b) and PLSC 2 (c-d) . Average batch trajectory, upper and lower control limits (CL) and the predicted trajectories of the four test batches (TB A – TB D) are shown. TB A and TB B are displayed in figures 7a and 7c. TB C and TB D are displayed in figures 7b and 7d.

Figure 8. Hotelling's  $T^2$  plot of reference PCA model for the test batches TB A – TB B (a) and TB C – TB D (b) respectively. Figure 9. Batch contribution plots of how test batch C and the average batch differ at time points 125 (a), 135 (b) and 165 (c) respectively.

Figure 10. PCA score plot showing the distribution of completed reference (B1 – B10) and test batches (TB A – TB D) with a confidence ellipse at significance level 0.05.

Figure 1.

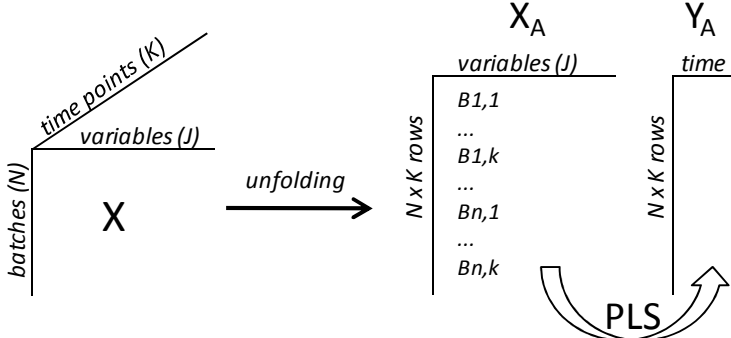


Figure 2.

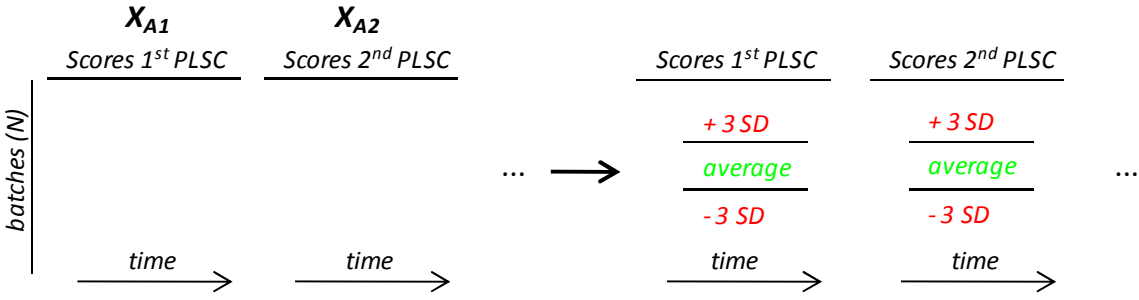


Figure 3

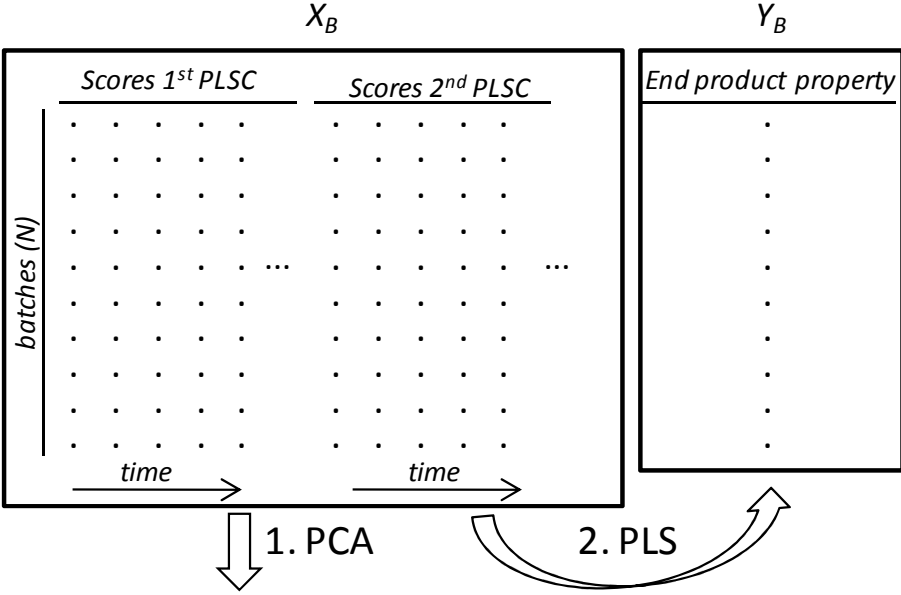


Figure 4.

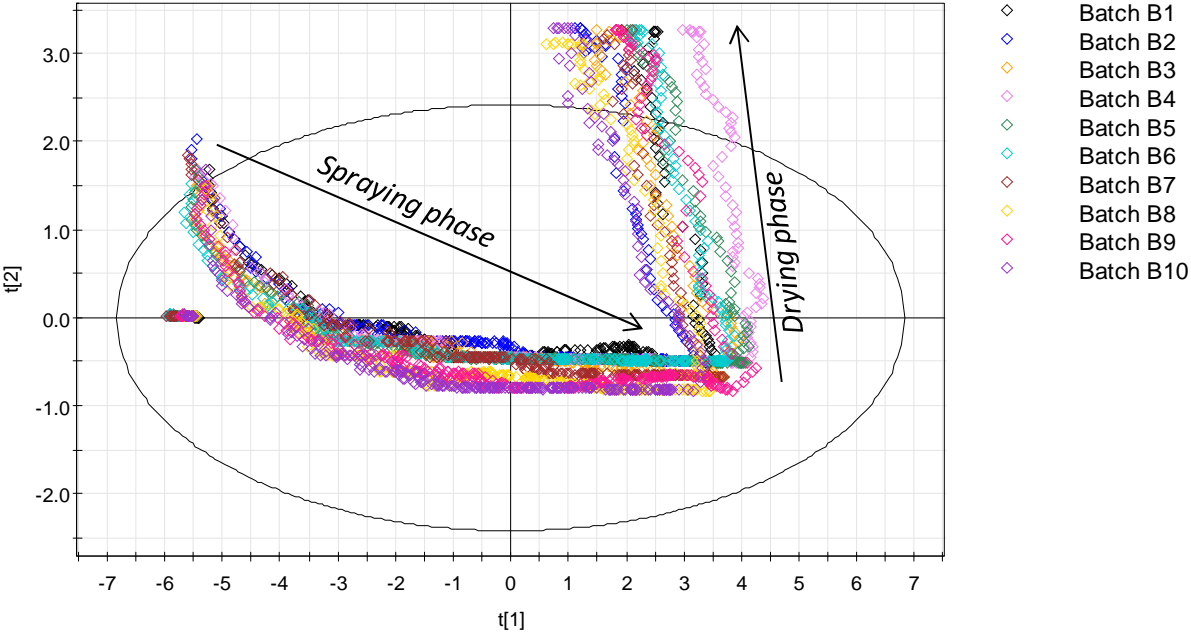


Figure 5a.

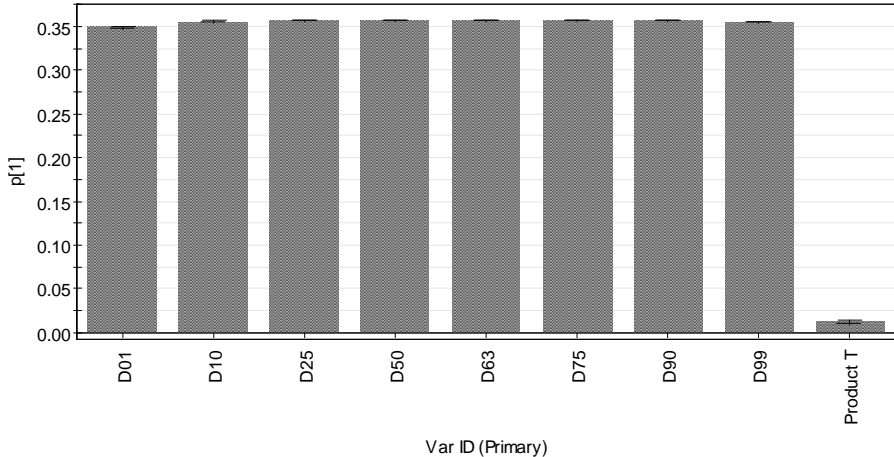


Figure 5b.

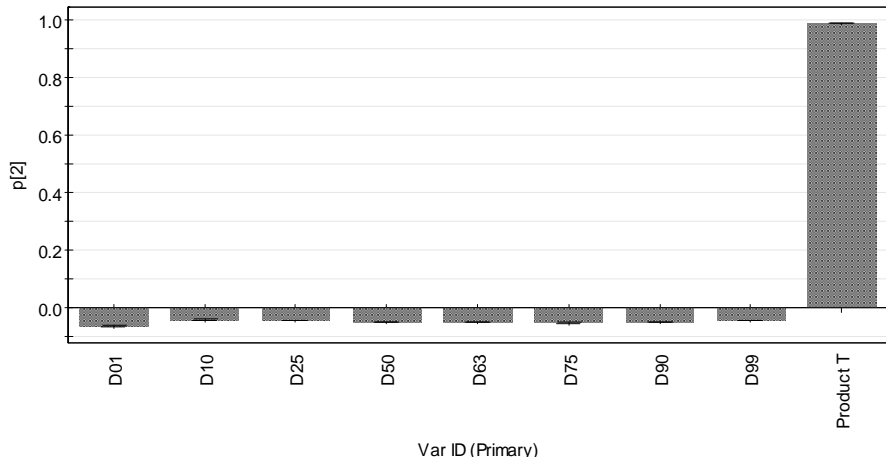


Figure 6a.

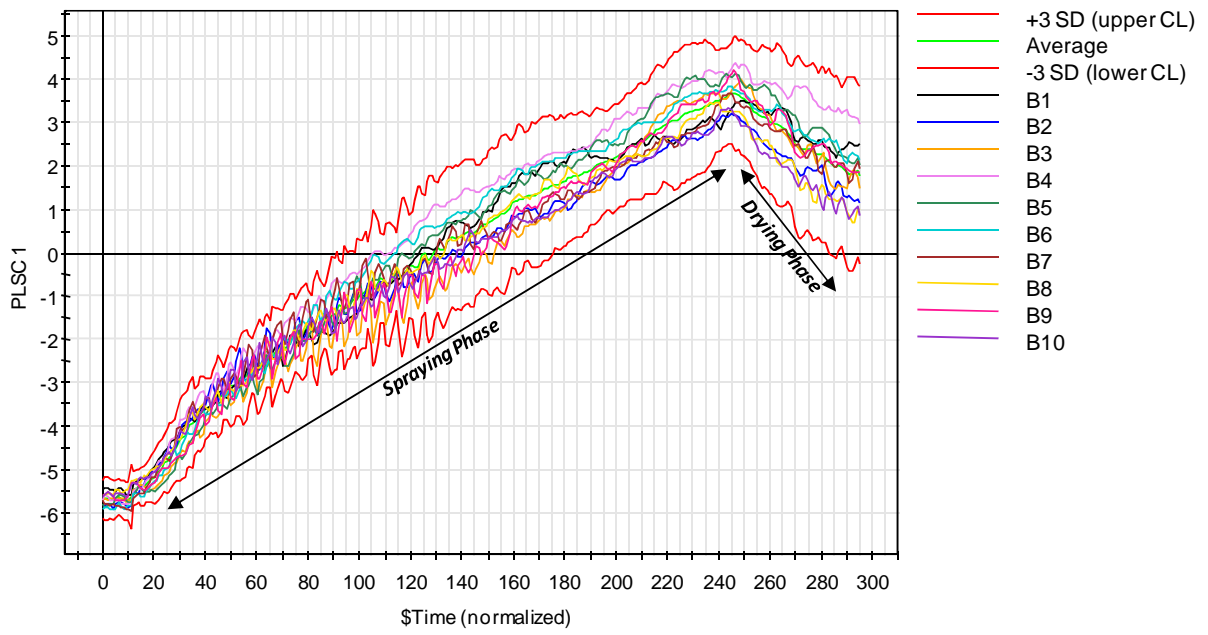


Figure 6b.

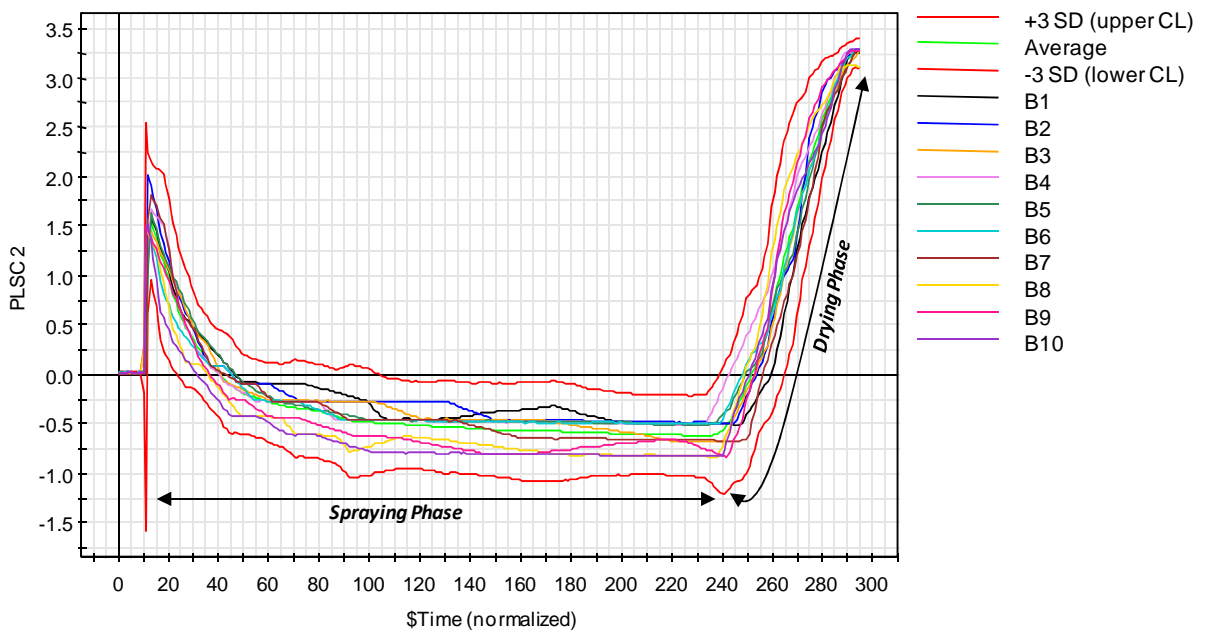


Figure 7.

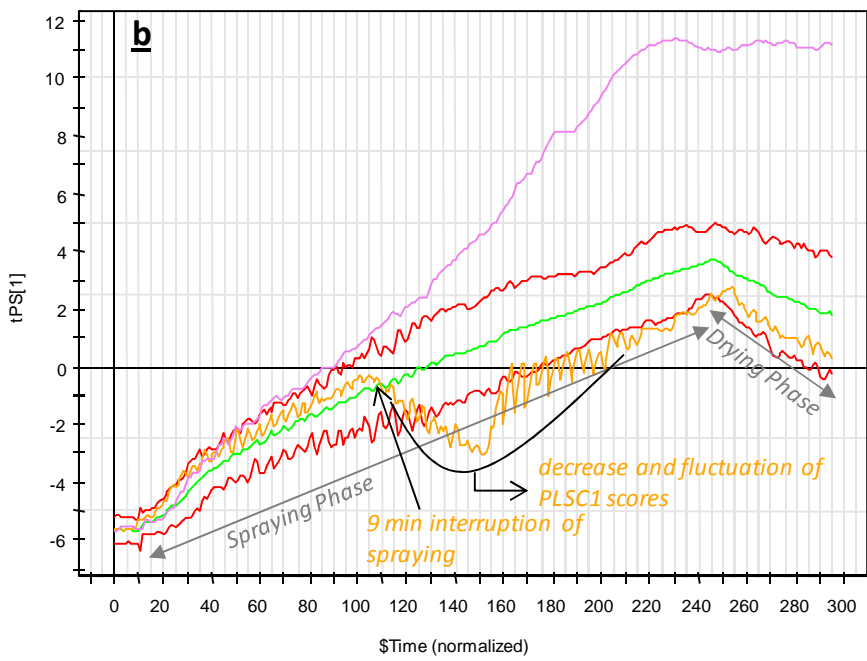
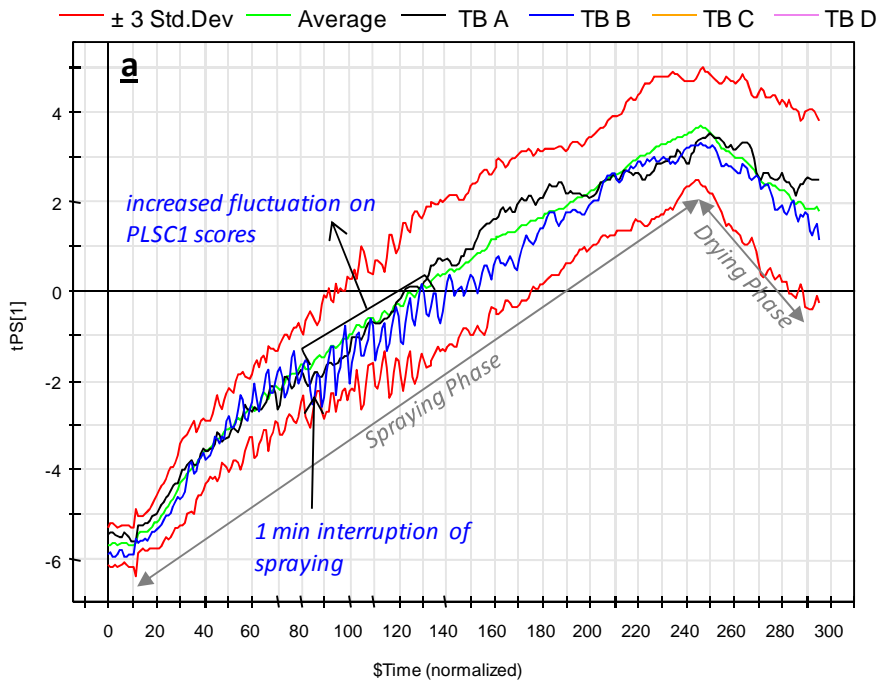


Figure 7.

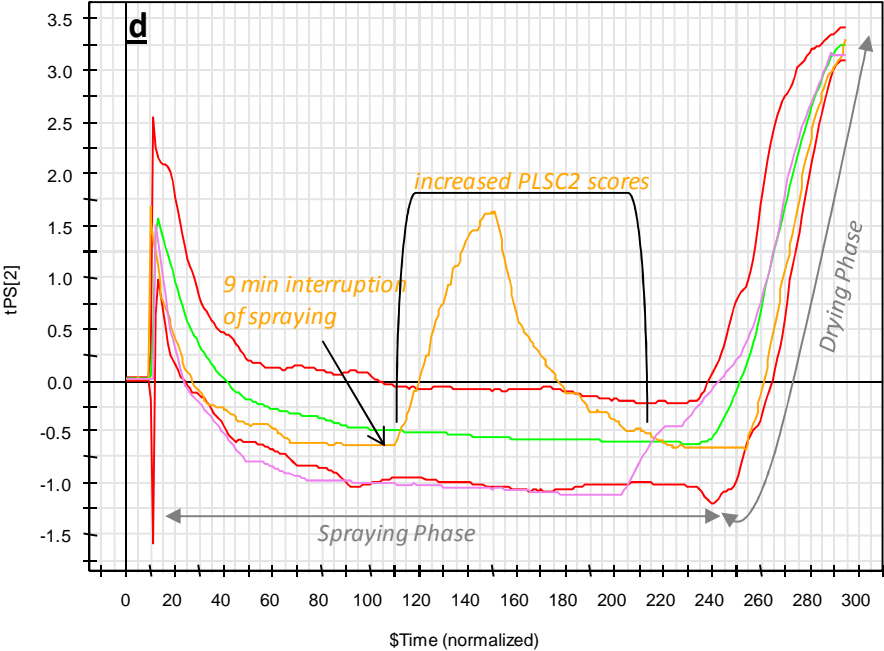
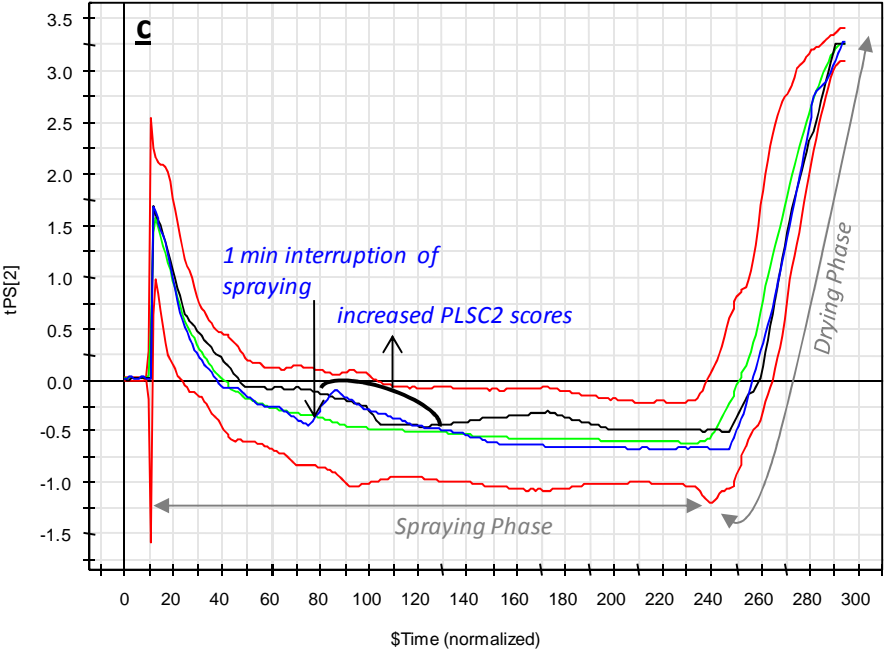


Figure 8.

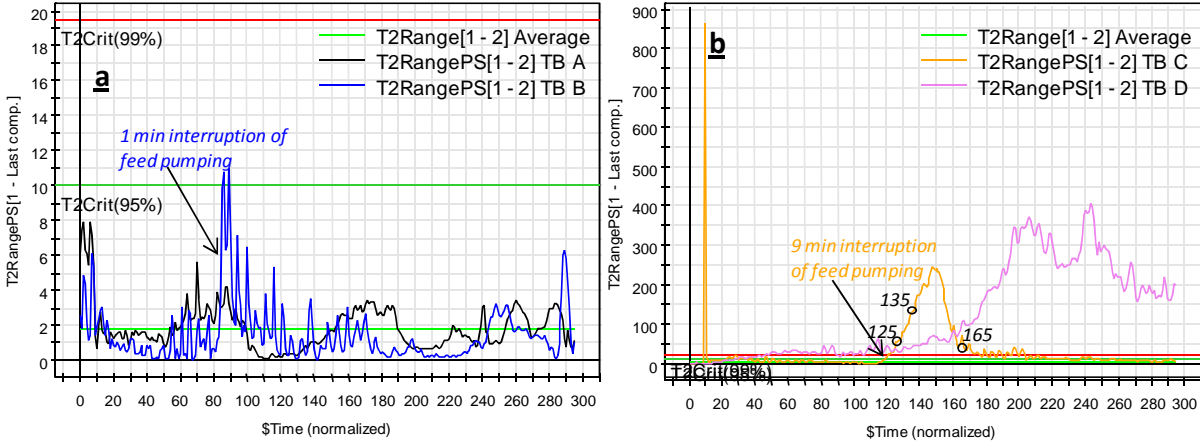


Figure 9.

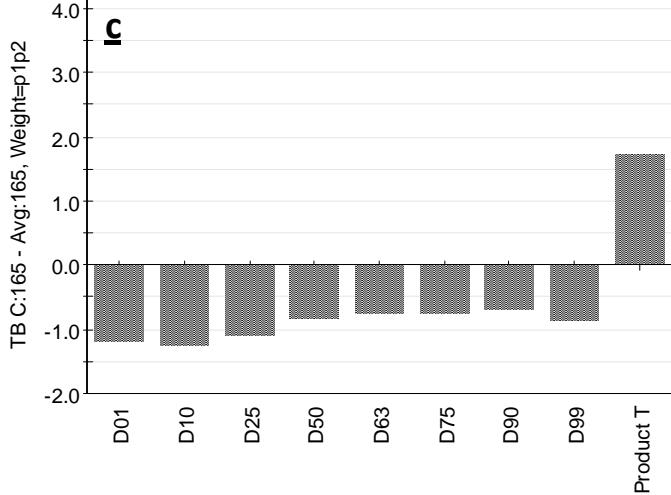
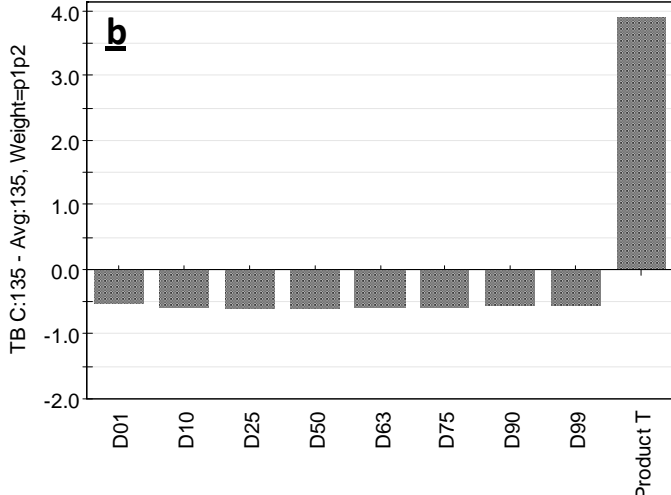
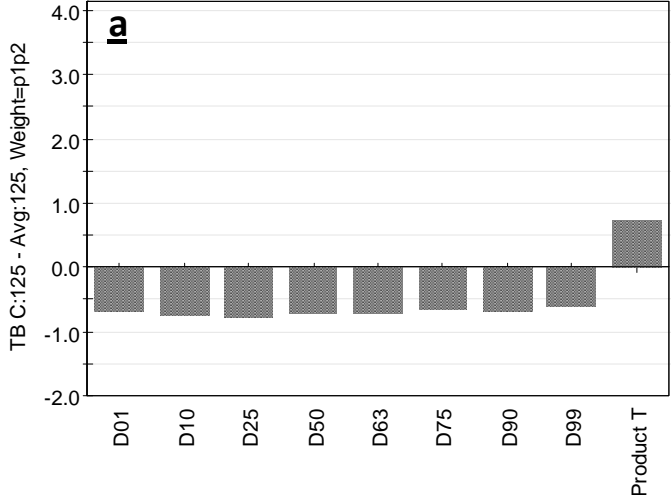


Figure 10.

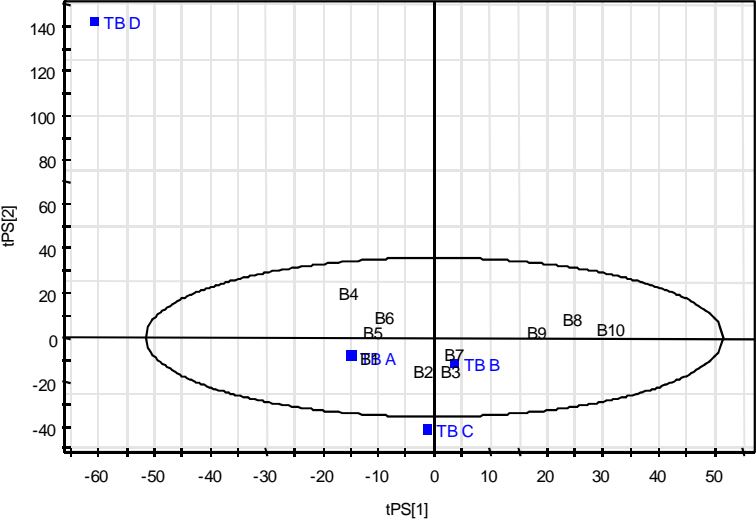


Table 1. Granulation conditions for test batches A, B, C, and D

name batch	Granulation conditions
TB A	Identical conditions as reference batches
TB B	Spraying of granulation liquid was stopped during 1 minute
TB C	Spraying of granulation liquid was stopped during 9 minutes
TB D	Rate of spraying granulation liquid was increased to 21 g/min

Table 2. End product particle size distribution, measured and predicted bulk density, tapped density and Hausner ratio according to whole batch PLS model for reference and test batches. Standard deviations were calculated for 3 replicates.

Batch	<i>Particle size distribution</i>			<i>Bulk density</i>		<i>Tapped density</i>		<i>Hausner ratio</i>	
	D10	D50	D90	measured	predicted	measured	predicted	measured	predicted
B1	150	293	510	$0.425 \pm 0.009$	0.425	$0.511 \pm 0.008$	0.510	1.203	1.204
B2	139	268	445	$0.370 \pm 0.003$	0.368	$0.447 \pm 0.002$	0.445	1.208	1.202
B3	137	283	481	$0.390 \pm 0.004$	0.391	$0.472 \pm 0.001$	0.476	1.211	1.216
B4	167	313	538	$0.399 \pm 0.003$	0.396	$0.470 \pm 0.003$	0.467	1.179	1.178
B5	147	295	492	$0.387 \pm 0.001$	0.396	$0.473 \pm 0.004$	0.480	1.222	1.218
B6	152	294	488	$0.391 \pm 0.001$	0.388	$0.468 \pm 0.005$	0.466	1.199	1.203
B7	145	288	486	$0.377 \pm 0.001$	0.376	$0.455 \pm 0.002$	0.455	1.208	1.205
B8	129	261	444	$0.411 \pm 0.003$	0.409	$0.492 \pm 0.006$	0.490	1.198	1.199
B9	142	288	482	$0.415 \pm 0.003$	0.410	$0.496 \pm 0.001$	0.491	1.195	1.198
B10	131	259	435	$0.394 \pm 0.006$	0.399	$0.477 \pm 0.003$	0.482	1.209	1.207
<b>TB A</b>	<b>148</b>	<b>290</b>	<b>515</b>	<b><math>0.425 \pm 0.005</math></b>	<b>0.420</b>	<b><math>0.511 \pm 0.006</math></b>	<b>0.505</b>	<b>1.203</b>	<b>1.198</b>
<b>TB B</b>	<b>99</b>	<b>223</b>	<b>413</b>	<b><math>0.390 \pm 0.001</math></b>	<b>0.379</b>	<b><math>0.478 \pm 0.002</math></b>	<b>0.462</b>	<b>1.224</b>	<b>1.215</b>
<b>TB C</b>	<b>97</b>	<b>222</b>	<b>408</b>	<b><math>0.383 \pm 0.005</math></b>	<b>0.330</b>	<b><math>0.472 \pm 0.003</math></b>	<b>0.407</b>	<b>1.231</b>	<b>1.211</b>
<b>TB D</b>	<b>275</b>	<b>513</b>	<b>849</b>	<b><math>0.456 \pm 0.009</math></b>	<b>0.507</b>	<b><math>0.525 \pm 0.002</math></b>	<b>0.563</b>	<b>1.151</b>	<b>1.111</b>